



## Intra-Articular Hyaluronic Acid and Chondroitin Sulfate: Pharmacokinetic Investigation in Osteoarthritic Rat Models

Massimiliano Fonsi, PhD, MSc<sup>1</sup>, Abdel-Ilah El Amrani, PhD<sup>2</sup>, Frédéric Gervais, DVM, ECVP<sup>3</sup>, Patrice Vincent, MEng<sup>4,\*</sup>

<sup>1</sup> DMPK, Citoxlab, Evreux, France

<sup>2</sup> Safety and General Pharmacology, Citoxlab, Evreux, France

<sup>3</sup> Citoxlab, Evreux, France

<sup>4</sup> LCA Pharmaceutical, Chartres, France

### ARTICLE INFO

#### Article history:

Received 24 September 2019

Accepted 3 December 2019

### ABSTRACT

**Background:** Viscosupplementation of synovial fluid with intra-articular (IA) injections of hyaluronic acid (HA) is widely used for symptomatic treatment of osteoarthritis (OA). Herein we present HCS, a new combination of chemicals, associating HA and chondroitin sulfate (CS), both members of the glycosaminoglycan (GAGs) family, which are major components of the joint. HA provides viscosity to the synovial fluid and CS provides elasticity to the cartilage. Reduced levels of HA and CS are observed in OA joints and are associated with progressive cartilage damage and loss.

**Objective:** The objective of the study was to evaluate the pharmacokinetic (PK) properties of both HA and CS after IA administration in a validated OA animal model.

**Methods:** Motion impairment measurements and histological examinations were used to validate the ability of an IA injection of mono-iodoacetate (MIA) in the knee of rats to induce OA symptoms. Then, the PK properties of HA and CS after IA administration were characterized and each active ingredient was independently profiled: HA was labeled with tritium (3H-HA) and CS was labeled with carbon 14 (14C-CS). The final radio-labeled solution reproduced the cold HCS formulation.

**Results:** Four male Sprague-Dawley rats received a 1 mg MIA injection on day 1, then motor impairment was monitored from day 4 to day 18. Chondrocyte necrosis, loss of GAGs and other cartilage damage were observed. Twelve other rats received a MIA IA injection on day 1 then a radio-labeled HCS IA injection (50 µL) on day 8. Plasma and knee cartilage were collected postadministration and the terminal half-life was similar in both matrices (about 5 days), for both 3H-HA and 14C-CS.

**Conclusions:** Despite differences in their molecular size, HA and CS showed PK behavior similarly characterized by prolonged residence inside the joint and slow release in plasma, favoring long-term beneficial effects. (*Curr Ther Res Clin Exp.* 2020; 92:XXX-XXX)

© 2019 LCA Pharmaceutical, Chartres, France. Published by Elsevier Inc.

This is an open access article under the CC BY-NC-ND license.

(<http://creativecommons.org/licenses/by-nc-nd/4.0/>)

### Introduction

Osteoarthritis (OA) is a painful and disabling disease affecting a large number of people older than age 50 years.<sup>1,2</sup> It is characterized by progressive cartilage degradation with loss of type II collagen and glycosaminoglycans (GAGs), which are normally present in the healthy joint,<sup>1</sup> in particular hyaluronic acid (HA),<sup>3</sup> the vis-

coelastic component of synovial fluid, and chondroitin sulfate (CS), a major component of the cartilage matrix.<sup>4,5</sup> HA is also present in the cartilage, where it contributes to formation of aggregates, which are large associations of proteoglycans.<sup>4</sup> The role of GAGs is essential. HA provides viscosity and elasticity to the synovial fluid (allowing lubrication and shock absorbance in the joint) due to its high molecular weight (MW), which is more than several million Daltons. Cartilage hydration and elasticity depend on the presence of CS. Other biological functions in the joint are also attributed to HA and CS.

The depletion of GAGs is therefore an important factor leading to accelerated cartilage degradation in the OA disease. The ability

\* Address correspondence to: Patrice Vincent, MEng, R&D, LCA Pharmaceutical, 9 allée Prométhée, F-28000, Chartres, France.

E-mail address: [pvincent@lca-pharma.com](mailto:pvincent@lca-pharma.com) (P. Vincent).

to self-repair cartilage is known to be very limited in young people, and almost absent in older people.<sup>4</sup> Although there is no established disease modifying agent for OA,<sup>4</sup> symptomatic treatments are proposed to alleviate pain and partially restore mechanical function. Among these treatments, viscosupplementation<sup>6–8</sup> of the synovial fluid with intra-articular (IA) injections of HA, has been widely used for several decades. The majority of exogenous HA remains in the joint for only a few days, but the clinical therapeutic effects of HA treatment may be seen for up to 6 months or more<sup>2,6–8</sup>; that is, several months after total clearance of the product. Because the administration local, viscosupplementation is considered as a safe treatment, free of systemic secondary effect.<sup>6–8</sup>

The presence of CS increases the tissue adherence properties when compared with an HA alone-based formulation. In this sense, a specific IA product formulation (Arthrum HCS or Synovium HCS from LCA Pharmaceutical, Chartres, France), combining both HA (20 mg/mL) and CS (20 mg/mL) may offer new therapeutic perspectives, but the exogenous IA CS with its smaller MW—<50 kDa—may be subject to a faster rate of elimination with respect to HA. In the absence of pharmacokinetic (PK) data in the literature, the exposure to the two GAGs (HA and CS) administered in combination needed to be directly measured and compared, both systemically and in the joint compartment. It was judged more relevant to carry out this study on an OA animal model to reproduce the influence of an altered joint context as in the case of a human knee with OA disease.

The objective of the study presented in this article was to evaluate the PK profiles of the radio-labeled test items: tritium-labeled HA (<sup>3</sup>H-HA) and carbon 14-labeled CS (<sup>14</sup>C-CS), administered in combination via a single IA (bolus) injection to an arthritis disease model developed in rats. The time profile of tritium- and carbon 14-associated radioactivity in the administration site and in plasma were measured. To validate this OA model before PK, evaluations of motor activities together with histopathology examinations of the knees were performed after mono-iodoacetate (MIA) injection in rats. This study was entirely performed at Citoxlab France (BP 563, 27005 Evreux, France), from 2016 to 2018.

## Methods

### *Ethical statement and animal welfare*

The study was conducted in compliance with animal health regulations, in particular Council Directive No. 2010/63/EU of September 22, 2010, on the protection of animals used for scientific purposes.

The Citoxlab France Ethical Committee (CEC)—accredited by the International Association for Assessment and Accreditation of Laboratory Animal Care—reviewed the present study plan to assess the compliance with the corresponding authorized project as defined in Directive 2010/63/EU. The CEC notified the study director of the review before the finalization of the study plan. During the study, the CEC was regularly informed of any amendments to the study plan that could affect animal welfare.

### *Receipt, identification, and acclimation*

On arrival, the animals were given a clinical examination to ensure that they were in good condition. Each animal was identified by an individual ear tattoo, then they received a unique Citoxlab identity number at the beginning of the study. The animals were acclimated to the study conditions for a period of 7 days before the beginning of the treatment period.

### *Housing and environmental conditions*

The animals were group housed (maximum 5 animals) in polycarbonate cages (2065 cm<sup>2</sup>) with stainless steel lids, containing autoclaved sawdust, nylabone, and a rat hut for the environmental enrichment of the animals. The animal room was controlled at 22°C ±2°C temperature, 50% ±20% relative humidity, 12-hour/12-hour light/dark cycle, and ventilated with filtered, nonrecycled air (8–15 cycles/hour).

### *Food and water*

All animals had free access to pelleted maintenance diet and tap water (filtered at 0.22 μm) in bottles. The batches of diet and sawdust were analyzed by the suppliers for composition and contaminant levels. Bacterial and chemical analyses of water were performed regularly by external laboratories. No contaminants were present in the diet, drinking water, or sawdust at levels that could have been expected to interfere with, or prejudice, the outcome of the study.

### *Part 1: Osteoarthritis model*

#### *MIA rat model*

The first step was selection of the method to induce OA in rats. Considering the risk of obtaining higher severity than for human OA, rather than using a surgical method such as anterior cross ligament (ACL) transection or meniscectomy, our preference was for OA induction by IA injection.<sup>9</sup> An OA model was initially set up based on the IA injection of MIA, a known technique that induces chondrocyte death in the articular cartilage of rodent and nonrodent species.<sup>10–23</sup> The rat model used in the present study was adapted from a method described by Guingamp et al.<sup>10,11</sup> A summary of available studies describing MIA-induced OA in the rat is given in Table 1. Among the different doses tested on animals, the lowest (≤0.3 mg) did not reach an appreciable impairment level within 7 days postinjection, whilst the highest (≥2 mg) led to irreversible damage that was too severe within a time as short as 14 days (Figure 1). After selection of an intermediate 1 mg MIA dose that was applied on day 1, OA symptoms were induced in rats a few days after administration.<sup>12</sup> The induced lesions were demonstrated by observing the OA symptoms during motor activity testing and by comparative joint histology. The remaining point was to optimize the time-lapse for potential OA treatment (IA intervention), as proposed in Figure 1. Relatively fast evolution of OA was expected after MIA injection. Consequently, a gap of a few days had to be left before the next intervention. This gap started after the earliest motor impairment in the animal and finished before any subchondral collapse.

Nine male Sprague-Dawley rats—Rj:SD (IOPS Han)—were included in this part of the study. These animals were trained for motor activity testing beforehand, including rearing and horizontal movements. Only trained animals were included in the group.

#### *MIA-treated group*

Five animals were anesthetized (using isoflurane) and received a single IA injection of 1 mg MIA (50 μL/injection at 20 mg/mL) through the patellar ligament between the tibia and femur of the right knee using a 27-gauge needle.

#### *Control group*

Four untreated animals were used as a control group to obtain comparative results on the physical assessment (ie, motor activity). These animals representing safe subjects, were the same species and age; similarly reared; and then submitted to the same initial training, follow-up, and testing as the MIA-treated group, except

**Table 1**  
Mono-iodoacetate (MIA) rat studies: Tabulated summary.

Study	Rat strain	Body weight (g) (age)	MIA injected			Observations*
			Volume ( $\mu$ L)	Dose level (mg)	Dose (mg/kg)	
Guingamp <sup>10,11</sup>	Wistar	150–225	50	0.3	1.6	Day 1–2: Activity reduced Day 3–6: Normal activity Day 7+: Activity reduced Rapid degradation
Janusz et al <sup>12</sup>	Sprague-Dawley	220–230	50	3	16	Day 1–7: Progressive GAG loss
Guzman et al <sup>13</sup>	Wistar	175–200	25	0.25	1.1	Day 21: Subchondral degradation
			50	1	5.3	Day 1: Chondrocytes degenerate Day 5–7: Cartilage and loss of chondrocytes Day 7–14: Subchondral bone marrow loss
Saito <sup>14</sup>	Wistar	(10–11 wk)	50	0.1	0.4	Day 28: Multiple collapse Weak damage by MIA
Peng et al <sup>15</sup>	Lewis	(old males)	50	1	4	Degradation, 15 km walk Day 3: Onset of pain, Day 14–28: Femorotibial and femoropatellar damages
Ferland-Legault <sup>16,17</sup>	Sprague-Dawley	180–225	30	3	15	Day 3, 7, 14, 21, 28: Structural damages Day 7–21: Similar to OA in human
Liu et al <sup>18</sup>	Sprague-Dawley	275–300	60	4.8	16	High doses have been deliberately selected
Mannelli et al <sup>19</sup>	Sprague-Dawley	200–250	25	2	8.9	<i>Day 0: Anti-O<sub>2</sub>- treatment</i> <i>Day 14: Slowed OA</i>
Benschop et al <sup>20</sup>	Wistar	8 (wk)	50	0.3	1.5	Day 14: MIA controls severely affected NSAID responders : <i>Day 14: Treatment</i> <i>Day 17: Pain evaluation</i>
			50	1	5	NSAID non-responders : <i>Day 40: Treatment</i> <i>Day 43: Treatment and pain evaluation at +2 h</i>
Naveen et al <sup>21</sup>	Sprague-Dawley	100–150 (12 wk)	25	2	16	Cartilage thickness and GAG Day 7: Moderate degradation Day 14: Major degradation
Calado et al <sup>22</sup>	Wistar	250	25	2	8	Day 3: Major handicap Study limited to 10 days
Jain et al <sup>23</sup>	Charles Foster	180–220	40	2	10	<i>Day 7–14: Oral diacerein</i> <i>Day 28: OA slowed</i> <i>Day 56: Cartilage healed</i> MIA controls: Day 7: Loss of hyalin cartilage Day 14: Deep fissures Day 28: Subchondral bone collapsed Day 56: Total loss of cartilage

GAG = glycosaminoglycan; O<sub>2</sub><sup>-</sup> = Superoxyde anion; OA = osteoarthritis; NSAID = non-steroidal anti-inflammatory drug

Observations are in italic characters for the groups receiving a treatment

\* MIA was injected on Day 0.

that they did not receive any injection. The interest of this post-hoc control group was to identify any factors (such as habituation) that could have an incidence on the test results and that were not directly related to the MIA effect.

All animals were checked for mortality, morbidity, and clinical signs at least once a day during the study, including weekends and public holidays. Any signs of pain and/or dysfunction (or impairment) were carefully recorded. The body weight of each surviving animal was recorded once before group allocation, before MIA administration and on day 4, day 8, day 11, day 15, day 18, and day 22, post treatment. The schedule for each animal is described in Table 2.

#### Motor activity

Pain or locomotor impairment in animals was evaluated from the measurement of physical activity. Daily observation completed the diagnosis, to evaluate the appearance, extent, and evolution of the OA symptoms in the MIA-injected rats.

Animals were not fasted or deprived of water before the test.

Motor activity (rearing and horizontal movements) was measured in MIA-treated animals and nontreated control animals by automated infrared sensor equipment from Imetronic (Pessac, France), over a 60-minute period. Measurements were performed in MIA-treated animals before treatment on day 1 and after treatment on day 4, day 8, day 11, day 15, and day 18. For nontreated animals, these measurements were performed on the same days as the MIA-treated animals.

#### Statistical analysis

Quantitative variables were described by their mean and SD at each observation time. Coefficient of variation (CV) percent, was also used. Whenever comparison between groups was possible, the difference of variation to baseline (MD) was assessed and completed with pooled standard deviation (SD<sub>p</sub>), then the effect size (ES = MD / SD<sub>p</sub>) and *p*-value were calculated.

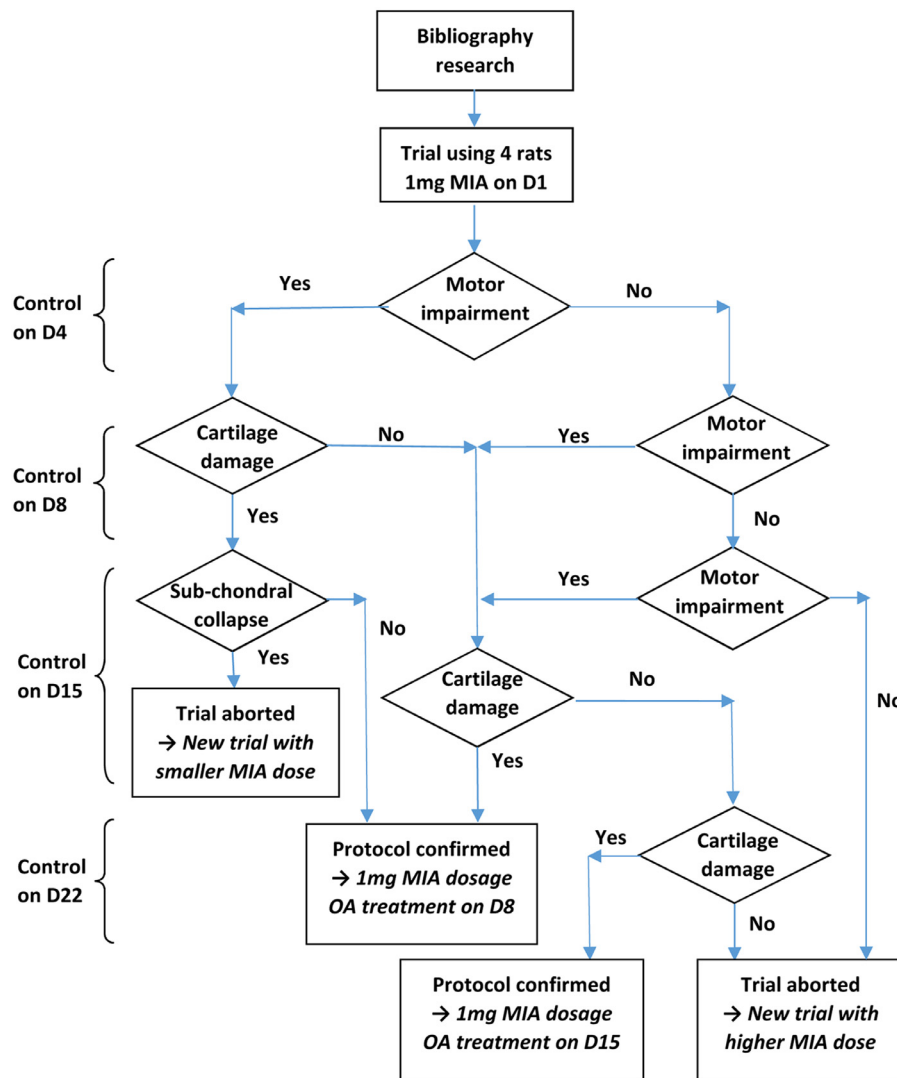


Figure 1. Rationale graph. D = day; OA = osteoarthritis; MIA = mono-iodoacetate.

Table 2  
Animal model motor activity schedule.

Group	Animal ID	Training day	Baseline treatment*	Follow-up day	Day of euthanasia	Comment
MIA	G23341	-4, -5	MIA	4, 8	8	Analyzed
	G23342	-4, -5	MIA	4, 8, 11, 15, 18	22	Analyzed
	G23343	-4, -5	MIA partial (<1 mg)	4, 8	8	Removed
	G23344	-4, -5	MIA	4, 8, 11, 15	15	Analyzed
	G23345	-4, -5	MIA	4, 8	9	Analyzed
Control	G23346	-3, -4	None	4, 8, 11, 15, 18	22	Analyzed
	G23347	-3, -4	None	4, 8, 11, 15, 18	22	Analyzed
	G23348	-3, -4	None	4, 8, 11, 15, 18	22	Analyzed
	G23349	-3, -4	None	4, 8, 11, 15, 18	22	Analyzed

Training, follow-up and put-to-death information are presented as study day. MIA = mono-iodoacetate.

\* Baseline treatment occurred on day 1.

## Pathology

Cartilage lesion was evaluated by comparative histological examinations of MIA injected knees and noninjected opposite knees in treated animals. In the MIA group, one animal was euthanized on day 8 (G23341), one on day 9 (G23345), one on day 15 (G23344), and another on day 22 (G23342), as shown in Table 2. Animals were deeply anesthetized by an intraperitoneal injection of sodium pentobarbital and sacrificed by exsanguina-

tion. Macroscopic examination, tissue processing, histological slide preparation and microscopic examination were all performed at Citoxlab.

Control animals were euthanized at the end of the experimental phase (day 22). No macroscopic or microscopic post mortem examinations were performed and no tissues were preserved in this group. These nontreated animals were deeply anesthetized by an intraperitoneal injection of sodium pentobarbital, euthanized by cervical dislocation, and discarded.

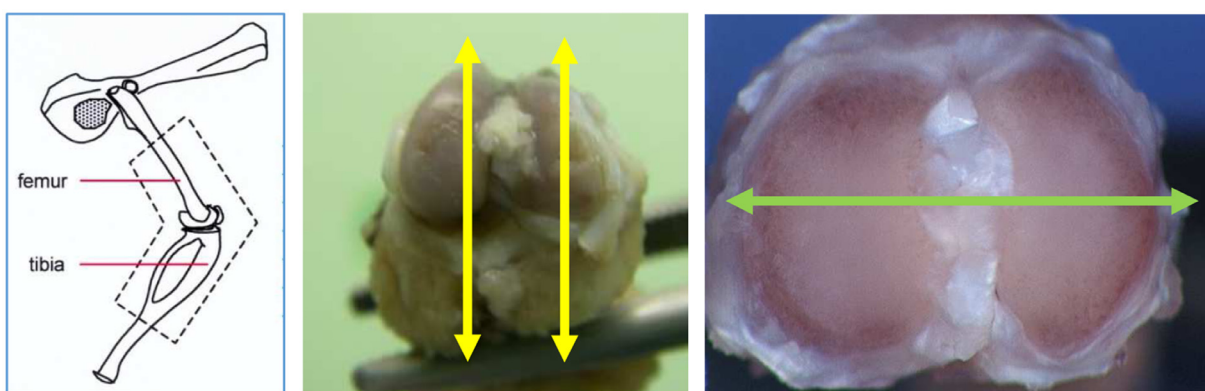


**Figure 2.** Cross-sectioning positions: longitudinal (yellow arrows) and transversal (green arrow).

#### Macroscopic postmortem examination

Macroscopic examination of the right and left femorotibial joints was performed for animals euthanized on day 8 (G23341), day 9 (G23345), day 15 (G23344), or day 22 (G23342). Photographs of right and left knees of animals euthanized on day 9 (G23345) or day 22 (G23342) were taken for macroscopic examination after indian ink staining.

#### Preservation of tissues

For all MIA-injected animals, the right and left femorotibial joints were preserved in 10% buffered formalin.

#### Preparation of histological slides

Both femorotibial joints (including the articular cartilage) were trimmed according to the Registry of Industrial Toxicology Animal-data guidelines,<sup>24–26</sup> embedded in paraffin wax, sectioned at a thickness of approximately 4  $\mu\text{m}$ , and stained with hematoxylin and eosin (H&E) or with safranin O (to enhance the GAGs). The samples were sectioned longitudinally (Figure 2) for animals euthanized on day 8 (G23341) or day 15 (G23344). A total of 4 histological slides of femur and 4 of tibia (4 with H&E and 4 with safranin O staining) were prepared from the right and left knees of these animals. For the animals euthanized on day 9 (G23345) or day 22 (G23342), 2 step sections, 150  $\mu\text{m}$  apart, were prepared according to the transverse sectioning angle (Figure 2) in the tibial plate: 4 slides were made for each level (2 were stained with H&E and 2 with safranin O).

#### Microscopic examination

Microscopic examination of articular cartilage was performed on left and right knees of each animal euthanized on day 8, day 9, day 15, or day 22. Commented photographs were provided.

#### Part 2: Pharmacokinetics

##### Radio-labeled preparation

The objective of this phase of the study, was to investigate the PK behavior of the HA and CS. A formulation containing  $^3\text{H}$ -HA and  $^{14}\text{C}$ -CS, reproducing the original formula of the HCS solution, was prepared. Cold ingredients HA and CS (as powders) and the buffered saline solvent as used for the HCS formulation were supplied by LCA Pharmaceutical. The active ingredients were radiolabeled at Quotient Bioresearch (Cardiff, United Kingdom). Briefly, each individual polysaccharide was partially de-acetylated and reconverted to the starting degree of acetylation by reactions with radiolabeled acetic anhydride. Two preparations were synthesized, 1 containing  $^3\text{H}$ -HA and the other  $^{14}\text{C}$ -CS, in the same saline-buffered solvent, and 5 mCi of each radio-labeled component were

obtained. Size exclusion chromatography (SEC) confirmed quantitatively the presence of each polymer. The cold starting material, HA and CS polymers, were used as reference marker respectively for  $^3\text{H}$ -HA and  $^{14}\text{C}$ -CS in the HPLC-SEC analysis. The retention time suggested a low MW for  $^3\text{H}$ -HA. However, previous studies revealed that basic pathways of distribution of HA molecules and its breakdown products showed only slight differences in the behavior of molecules of different MWs in the rat model<sup>27</sup>. For this reason, the obtained PK results in this study were considered representative of the HA and CS in the original pharmaceutical preparation.

These radio-labeled ingredients were mixed with HA and CS cold active ingredients at Citoxlab to precisely reproduce the original HCS formulation obtained from LCA Pharmaceutical (ie, 20 mg/mL for total HA and 20 mg/mL for total CS), each at a convenient radioactivity level. Because there was no evidence that this mixed HCS radio-labeled preparation could have the same clinical effect as a cold only preparation, no clinical assessment was planned on PK animals.

##### PK procedure

Following the preparation of the radio-labeled HCS solution, the PK study (including the in vivo phase, bioanalysis, and PK interpretation) was performed at Citoxlab. To provoke arthritis-like impairments, 12 male Sprague-Dawley rats received a single 50- $\mu\text{L}$  IA injection of 1 mg/animal MIA in the right knee on day 1. Then on day 8, all animals received a single IA (bolus) injection containing 1 mg each active ingredient (an isotopic mixture of cold HA and CS and radio-labeled  $^3\text{H}$ -HA and  $^{14}\text{C}$ -CS) in the articulation previously treated with MIA, under a total dose volume of 50  $\mu\text{L}$ .

Samples for the determination of  $^3\text{H}$ -HA and  $^{14}\text{C}$ -CS radioactivity in plasma and knee articulation were collected as follows:

- Plasma: 0.25 hour, 0.5 hour, 1 hour, 3 hours, 6 hours, 24 hours, 48 hours, 72 hours, 96 hours, 168 hours, 240 hours, and 336 hours after administration; and
- Knee: 6 hours, 24 hours, 240 hours, and 336 hours after administration.

The plasma CS and HA levels and the residual concentrations in the treated joint were monitored via Liquid scintillation counting (LSC). The energy spectrum differences of the beta particles emitted by each radio isotope were used to quantify total HA-related radioactivity and total CS-related radioactivity separately in each sample.<sup>28</sup>

The joint cartilage was collected at time of sacrifice following the terminal blood sample collection in each rat. The total radioactivity levels of  $^3\text{H}$ -HA or  $^{14}\text{C}$ -CS in plasma and right knee articulation were determined. Each individual isotope was quantified independently, in the same sample, directly after the addition

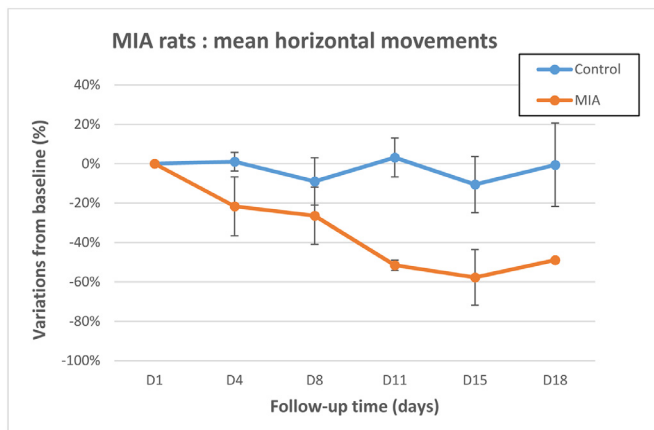


**Figure 3.** Motor activity I: Horizontal movements. Control group: n=4 animals at all time points. Mono-iodoacetate (MIA)-treated animals: n=4 up to day 8, n=2 on day 11 and day 15, and n=1 on day 18. Error bars represent SE. Difference is significant at day 11.

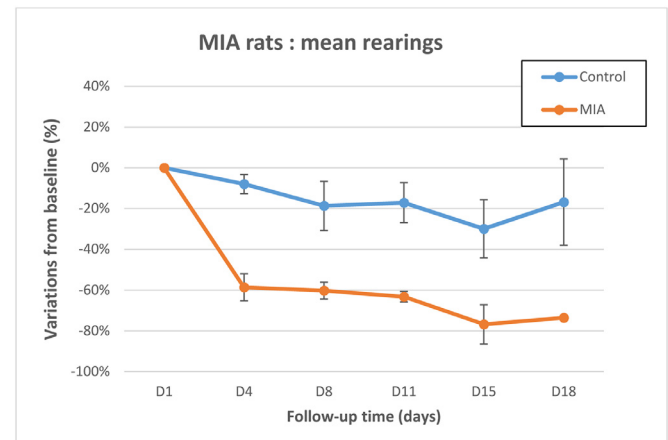


**Figure 4.** Motor activity I: Rearing. Control group: n=4 animals at all time points. Mono-iodoacetate (MIA)-treated animals: n=4 up to day 8, n=2 on day 11 and day 15, and n=1 on day 18. Error bars represent SE. Difference is significant from day 4 to day 15.

of liquid scintillation for plasma, or after cartilage digestion using 1 M sodium hydroxide followed by LSC (2 aliquots were analyzed for each digested tissue and the average value of the duplicate analysis was used for the PK analysis). As scintillation cocktail, Ultima Gold (PerkinElmer, Waltham, Massachusetts), was used (using 10 equivalent plasma or homogenate volumes per sample). A Tri-carb 2910TR Liquid Scintillation System (PerkinElmer) was used for the radio-detection.

#### PK analysis and statistics

After quantification of carbon 14 or tritium total related radioactivity by LSC, for each active ingredient (HA or CS), the relative PK parameters in plasma and knee articulation were determined in each matrix collected using the mean concentration profiles of 3 rats per time point. The following PK parameters were calculated: maximal concentration ( $C_{max}$ ), with corresponding time ( $T_{max}$ ), concentration at time zero (C0), time constant elimination ( $\lambda_z$ ), half life ( $t_{1/2}$ ), area under the curve at various time intervals ( $AUC_{0-t}$ , and  $AUC_{0-\infty}$ ). To complete an estimation was made of the 90% CI for the  $t_{1/2}$  of  $^3H$ -HA and  $^{14}C$ -CS in joint or plasma, using R version 3.6.1 software (R Foundation for Statistical Computing, Vienna, Austria).

## Results

#### Animal OA model

On the first day of treatment, the MIA-treated animals had a mean (SD) body weight of 253 (6) g (range, 248–262 g). For the control group, the mean (SD) body weight was 280 (5) g (range, 274–287 g) at inclusion in the study. This difference was not considered critical as no treatment was performed on control animals. Normal increases in body weight were observed throughout the study in all animals (reaching between 414 g and 442 g on day 21 or day 22). Among animals treated, 1 (G23343) received an incomplete injection of MIA, so it was removed from the analysis (Table 2).

Motor activity was assessed using infrared detection (Table 3, Figures 3 and 4). Decreased horizontal movement and rearing scores were observed in all MIA-treated animals from day 4 to day 18. Comparison of the mean variations to baseline revealed a significant difference ( $P < 0.05$ ) at day 11 for the horizontal movements, and from day 4 to day 18 for the rearing scores, confirming animal impairment in the MIA-treated group. ES was always found

from 0.76 to 5.14 for motor activity, which is quantitatively important because it is close or largely over 0.8, accordingly to Cohen<sup>29</sup>.

At the histology examinations performed on day 8, day 9, day 15, and day 22, there was evidence of MIA-induced degenerative OA, which was characterized by thickening of the synovial lining by inflammatory cells, necrosis and loss of chondrocytes in the articular cartilage, loss of GAGs, and also formation of clefts.

On day 15 and day 22, trabecular bone remodeling in the subchondral bone and release of eroded cartilage into the joint articular space were observed. There were signs of complete loss of proteoglycans in several articular plate areas, as suggested by safranin O staining.

Taken together, these results indicate that single IA injection of MIA (1 mg/animal) resulted in degenerative OA-like changes a few days after injection, associated with decreases in horizontal movement (Figure 3) and rearing (Figure 4) scores, but without any other clinical sign or mechanical dysfunctions.

#### Histology detailed results in MIA-treated rats

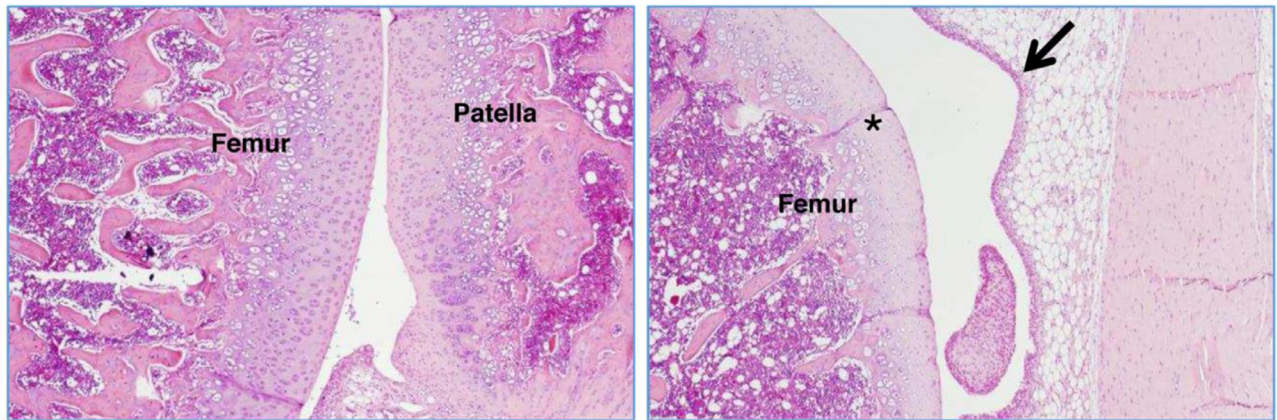
The right and left tibiofemoral joints of rat G23341 euthanized on day 8 and of rat G23344 euthanized on day 15 were examined microscopically. A longitudinal section through the femur, knee joint, and tibia (anteroposterior) was performed (Figure 2).

In rat G23341, there was evidence of induced degenerative OA, characterized by thickening of the synovial lining by inflammatory cells (Figures 5 and 6), necrosis and loss of chondrocytes in the articular cartilage (Figures 5–8), and formation of clefts (Figure 7). There was a marked decrease of safranin O staining in the affected areas, suggesting loss of proteoglycans and GAGs (HA and CS) (Figure 8).

In rat G23344, similar lesions to those shown in rat G23341 were observed (Figures 9–11). In addition, evidence of trabecular bone remodeling was noted (Figure 9), as well as release of eroded cartilage into the joint articular space (Figure 10). This was consistent with more prolonged insults to the articular surfaces. There were signs of complete proteoglycan loss in some areas, as suggested by the loss of safranin O staining (Figure 11).

In summary, degenerative changes were identified in the articular cartilages and lining synovial membranes from these 2 rats. The lesions were more severe and advanced in animal G23344 (day 15) than in animal G23341 (day 8).

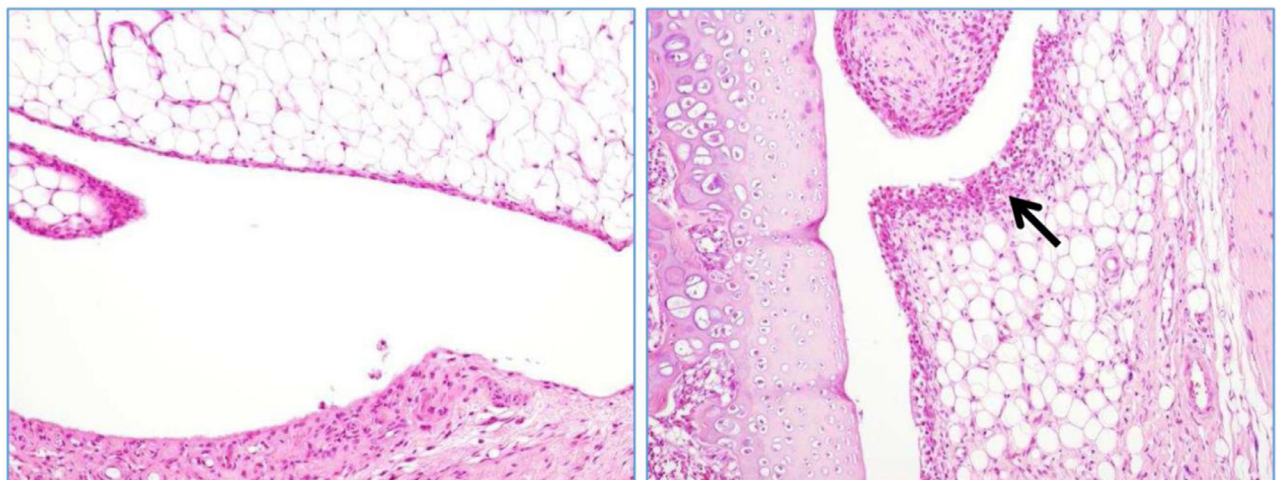
Knee articulation samples from rats G23345 and G23342, which were euthanized on day 9 and day 22, respectively, were



Control tibio-femoral joint, x40

Injected tibio-femoral joint, x40

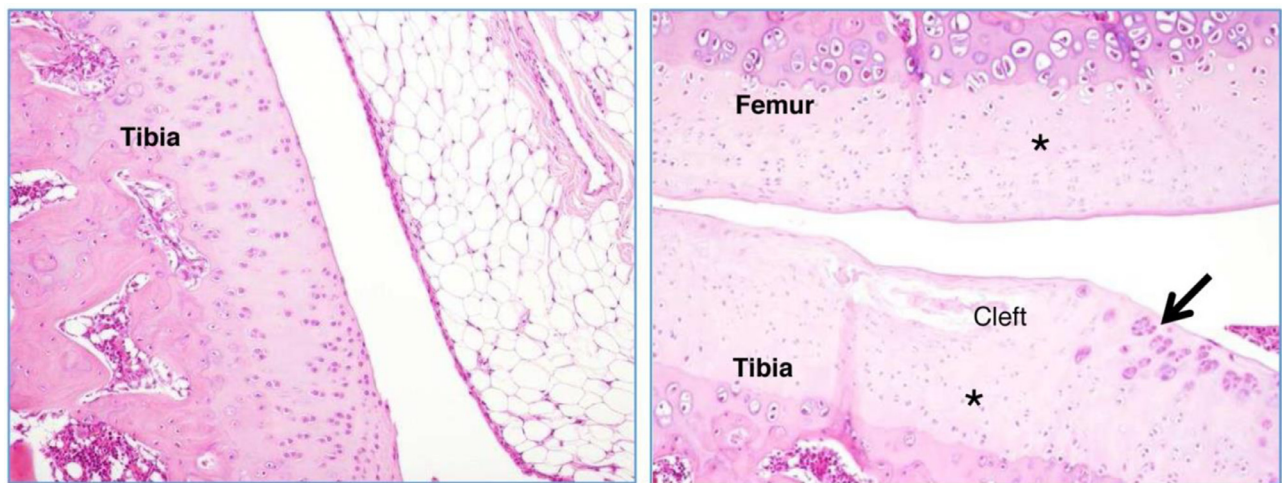
**Figure 5.** Rat G23341 (day 8). Comparison of right versus left (control) tibiofemoral joints. The arrow denotes synovial membrane thickening by inflammatory cells. The asterisk denotes area where chondrocyte density is decreased.



Control joint, synovial membrane, x100

Injected joint, synovial membrane, x100

**Figure 6.** Rat G23341 (day 8). Comparison of right versus left tibiofemoral joints. The arrow denotes thickening of the synovial lining by inflammatory cells.



Control tibio-femoral joint, x100

Injected tibio-femoral joint, x100

**Figure 7.** Rat G23341 (day 8). Comparison of right versus left tibiofemoral joints. Higher magnification reveals cartilage fibrillation and necrosis with a severe loss of chondrocytes for both tibial and femoral plates (denoted by asterisks). In the superficial layers, a cleft is seen in the tibial plate, and the arrow denotes clusters of proliferative chondrocytes.

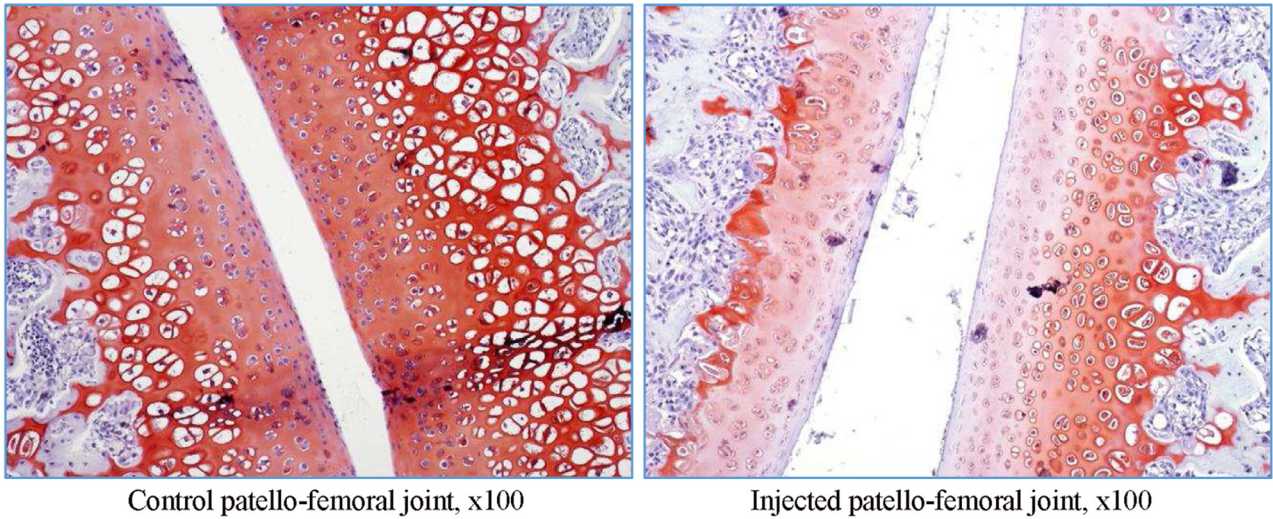


**Figure 8.** Rat G23341 (day 8). Comparison of right versus left tibiofemoral joints. Safranin O staining reveals the loss of proteoglycans along with decrease and thinning in the superficial cartilage matrix.

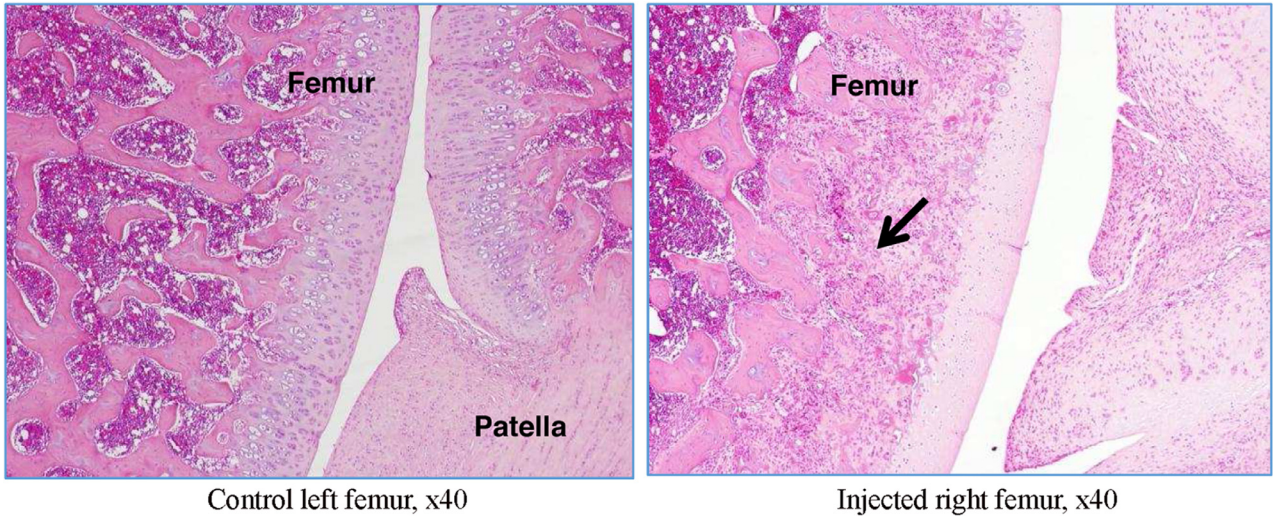


**Figure 9.** Rat G23344 (day 15). The trabeculae of the subchondral bone show variable degrees of thickening and remodeling (denoted by arrow).

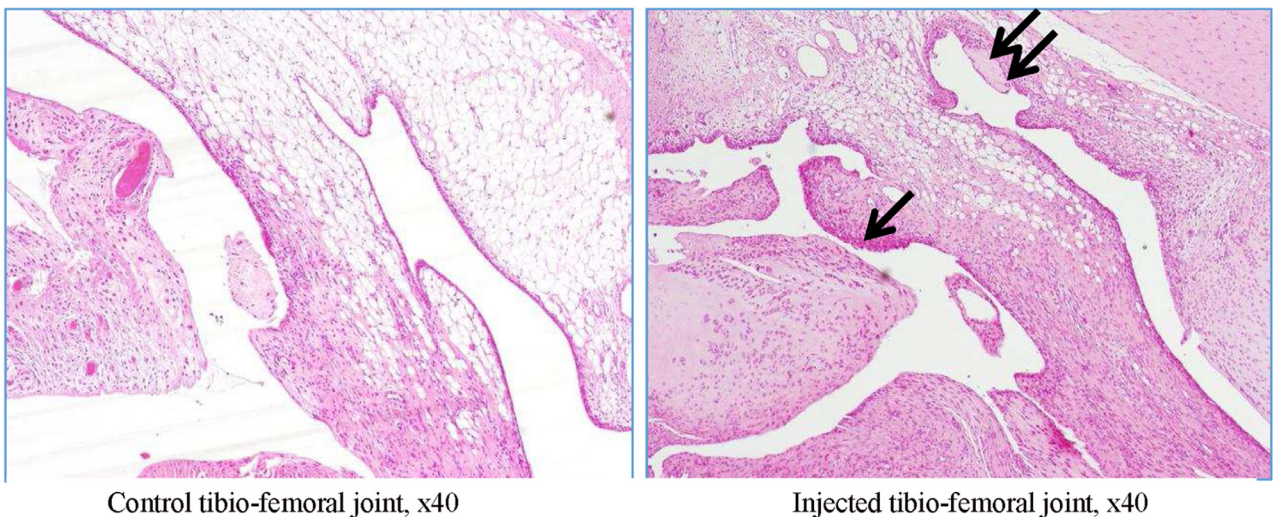


**Figure 10.** Rat G23344 (day 15). Hypertrophic villi lined with plump synoviocytes and infiltrated with mononuclear inflammatory cells (denoted by arrow). Fragments of degenerated cartilage, presumably derived from the eroded articular surface, embedded in the synovium or attached to its surface (denoted by double arrow).

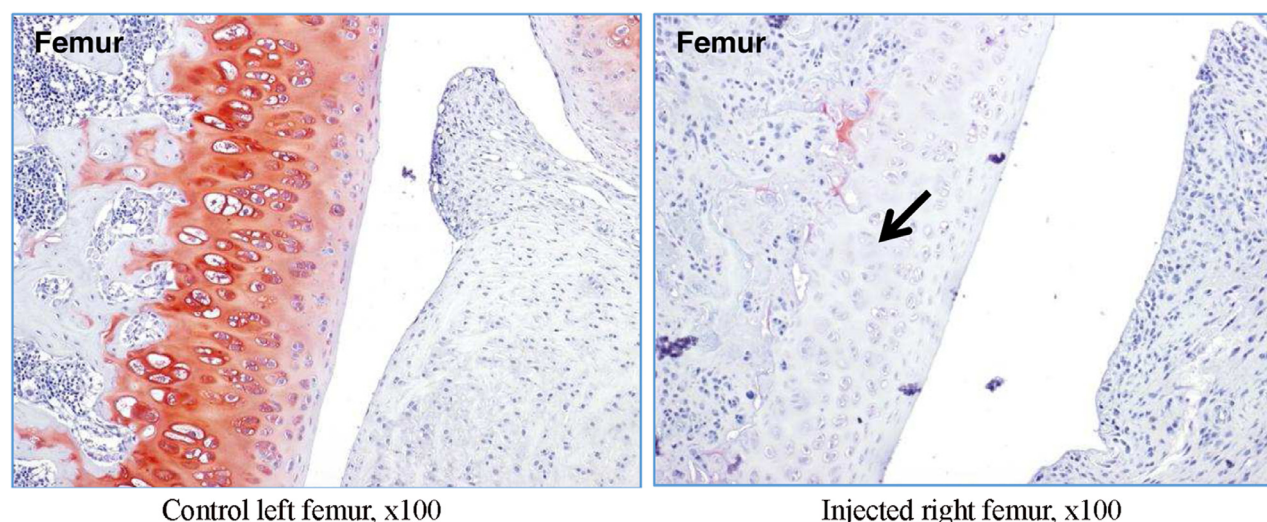


**Table 3**

Motor activity I: Automated infrared sensor.

Group	Animal ID	Day 1	Day 4	Day 8	Day 11	Day 15	Day 18
<b>Horizontal movements (scoring)</b>							
MIA	G23341	50	59	24			
	G23342	58	50	62	29	16	29
	G23344	53	49	47	26	32	
	G23345	66	20	34			
	Mean (SD)	56.8 (7.0)	44.5 (16.9)	41.8 (16.5)	27.5 (2.1)	24.0 (11.3)	29.0
Control	G23346	72	43	58	26	76	101
	G23347	53	50	42	75	26	41
	G23348	35	47	31	42	26	23
	G23349	29	51	41	52	41	23
	Mean (SD)	47.3 (19.4)	47.8 (3.6)	43.0 (11.2)	48.8 (20.5)	42.3 (23.6)	47.0 (37.0)
Comparison							
	Mean difference (pooled SD)	0 (14.6)	12.8 (12.2)	10.8 (14.1)	30.8 (17.8)	27.8 (21.2)	
	Effect size		1.04	0.76	1.73	1.31	
	P value		0.14	0.28	0.046	0.13	
<b>Rearings (scoring)</b>							
MIA	G23341	108	51	47			
	G23342	133	59	52	48	19	37
	G23344	161	83	73	55	46	
	G23345	159	39	51			
	Mean (SD)	140.3 (25.0)	58.0 (18.6)	55.8 (11.7)	51.5 (4.9)	32.5 (19.1)	37.0
Control	G23346	137	81	101	76	105	125
	G23347	79	80	89	52	54	82
	G23348	90	84	55	92	46	76
	G23349	68	99	59	90	57	28
	Mean (SD)	93.5 (30.4)	86.0 (8.8)	76.0 (22.5)	77.5 (18.4)	65.5 (26.7)	77.8 (39.7)
Comparison							
	Mean difference (pooled SD)	0 (27.8)	74.8 (14.5)	67.0 (18.0)	72.8 (16.2)	79.8 (25.0)	
	Effect size		5.14	3.73	4.50	3.18	
	P value		< 0.001	< 0.001	< 0.001	< 0.001	

MIA = mono-iodoacetate.

**Figure 11.** Rat G23344 (day 15). Loss of safranin staining on the superficial cartilage matrix, indicative of proteoglycan loss (denoted by arrow).

examined using transverse (left to right) sectioning as shown in Figure 2. Findings on the tibial plate confirmed focal necrosis of the cartilage leading to fissures (Figure 12) and remodeling of the subchondral bone (Figures 13 and 14). This was associated with marked decreased in safranin O staining (Figure 14).

#### Radio-labeled injections and in-life results

The specific activity of the isotopic mix in stock solutions and dose formulations is reported in Table 4.

The animals received 0.261 MBq/50  $\mu$ L of  $^3$ H-HA and 0.466 MBq/50  $\mu$ L of  $^{14}$ C-CS.

Per the planned schedule (Table 5), the 12 animals (identified: H23921–H23932) received MIA on day 1 then the HA and CS formulation on day 8 by IA injection. A good correspondence between the nominal dose volume and the actual administered volume was observed for the majority of the animals.

OA symptoms were considered to have been correctly induced in the animals by the MIA injection as locomotor difficulties were observed from day 4 to day 7.

Hematomas and swelling of the knees were observed from day 1 to day 4 after HA and CS administration. These clinical signs were considered to be due to the administration procedure. There was no mortality or morbidity during the study, and no analgesia was required.

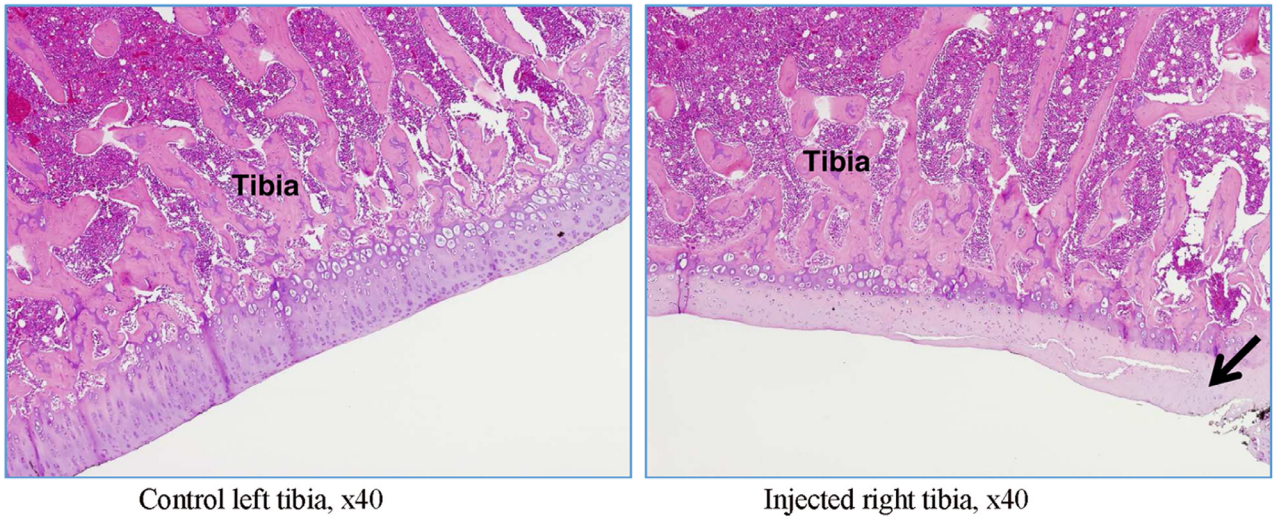


**Figure 12.** Rat G23345 (day 9). Comparison of right versus left tibia (transverse section). There is evidence of cartilage thinning and necrosis (denoted by arrow), leading to cracks. Subchondral bone seems to be nearly unchanged.

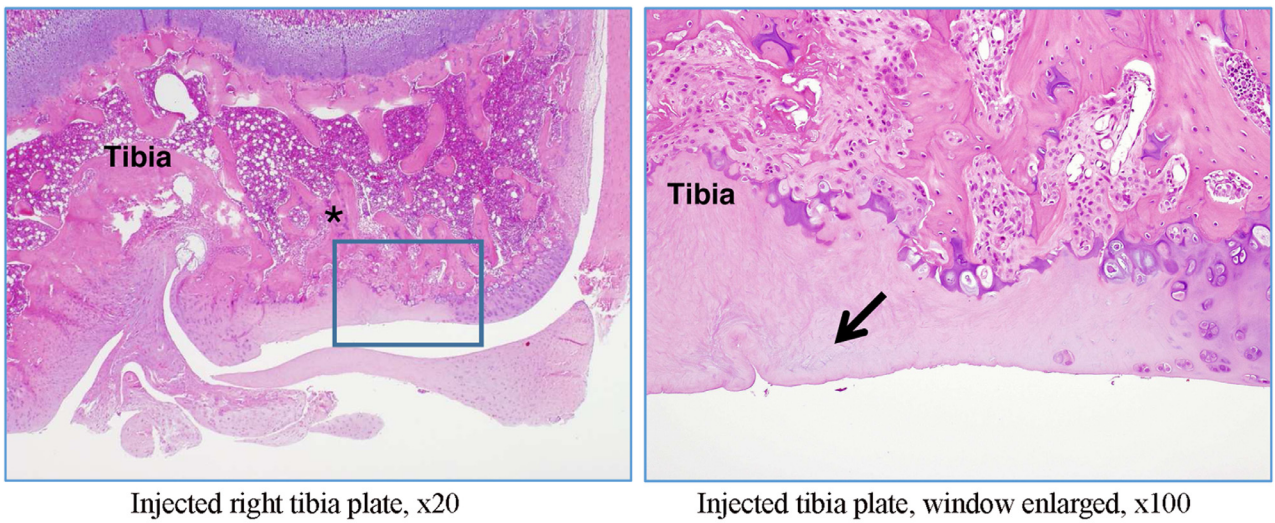


**Figure 13.** Rat G23342 (day 22). Right tibia (transverse section). The trabeculae of the subchondral bone show variable degrees of thickening and/or remodeling and a loss of hematopoietic cells (denoted by asterisk). The arrow denotes focal necrosis of the articular plate cartilage.

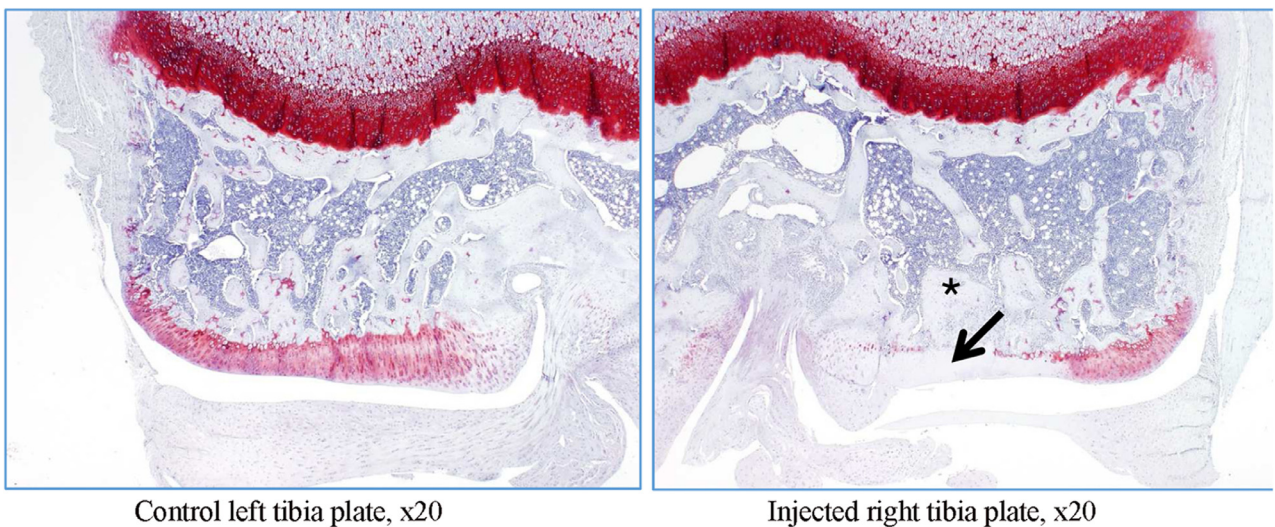


**Figure 14.** Rat G23342 (day 22). Comparison of right versus left tibia (transverse section). Marked decrease in safranin O positive area showing proteoglycan loss (cartilage necrosis) as denoted by an arrow. Subchondral bone shows variable degrees of remodeling and loss of hematopoietic cells (denoted by asterisk).

**Table 4**  
Radio-labeled preparation and injection.

ID number, sex, and identity of animals	Radioactivity <sup>3</sup> H-HA MBq/kg (MBq/50 µL)	Radioactivity <sup>14</sup> C-CS MBq/kg (MBq/50 µL)	Dose-level of each test item (mg/articulation)	Concentration each test item (mg/mL)	Day of administration
12 males: H23921 to H23932	2.45* (0.491)	1.30* (0.261)	1	20	8

<sup>14</sup>C-CS = carbon 14-labeled chondroitin sulfate<sup>3</sup>H-HA = tritium-labeled hyaluronic acid.

\* Calculated for a 200-g animal.

**Table 5**  
Individual concentration of tritium-labeled hyaluronic acid-related radioactivity (µg-eq/g) in plasma.

Animal ID	Sampling time (h)											
	0.25	0.5	1	3	6	24	48	72	96	168	240	336
H23921	0.585		1.17		2.13							
H23922	0.594		1.99		4.14							
H23923	0.685		1.44		4.40							
H23924		0.792		2.43		7.80						
H23925		1.01		2.40		7.11						
H23926		0.864		2.09		7.50						
H23927							5.53		3.84		1.37	
H23928							5.36		3.75		1.54	
H23929							6.71		4.54		1.50	
H23930								4.64		2.43		0.935
H23931								4.43		2.21		0.757
H23932								5.99		2.73		0.954
<b>Mean</b>	<b>0.620</b>	<b>0.887</b>	<b>1.53</b>	<b>2.31</b>	<b>3.56</b>	<b>7.47</b>	<b>5.87</b>	<b>5.02</b>	<b>4.04</b>	<b>2.46</b>	<b>1.47</b>	<b>0.882</b>
<b>SD</b>	<b>0.053</b>	<b>0.109</b>	<b>0.414</b>	<b>0.190</b>	<b>1.24</b>	<b>0.342</b>	<b>0.736</b>	<b>0.847</b>	<b>0.430</b>	<b>0.257</b>	<b>0.09</b>	<b>0.109</b>
<b>SE</b>	<b>0.031</b>	<b>0.063</b>	<b>0.239</b>	<b>0.110</b>	<b>0.72</b>	<b>0.197</b>	<b>0.425</b>	<b>0.489</b>	<b>0.248</b>	<b>0.148</b>	<b>0.052</b>	<b>0.063</b>
<b>CV</b>	<b>9%</b>	<b>12%</b>	<b>27%</b>	<b>8%</b>	<b>35%</b>	<b>5%</b>	<b>13%</b>	<b>17%</b>	<b>11%</b>	<b>10%</b>	<b>6%</b>	<b>12%</b>

**Table 6**  
Individual concentration of carbon 14-labeled chondroitin sulfate-related radioactivity (µg-eq/g) in plasma.

Animal ID	Sampling time (h)											
	0.25	0.5	1	3	6	24	48	72	96	168	240	336
H23921	3.29		3.43		0.705							
H23922	3.74		5.87		0.617							
H23923	3.88		5.38		0.790							
H23924		4.08		0.855		0.394						
H23925		5.03		1.14		0.338						
H23926		4.35		1.13		0.317						
H23927							0.164		0.0791		0.0128	
H23928							0.163		0.0777		0.0177	
H23929							0.187		0.0976		0.0180	
H23930								0.120		0.0325		0.00917
H23931								0.118		0.0348		0.00817
H23932								0.163		0.0410		0.0109
<b>Mean</b>	<b>3.64</b>	<b>4.49</b>	<b>4.90</b>	<b>1.04</b>	<b>0.704</b>	<b>0.350</b>	<b>0.171</b>	<b>0.134</b>	<b>0.0848</b>	<b>0.0361</b>	<b>0.0162</b>	<b>0.0094</b>
<b>SD</b>	<b>0.307</b>	<b>0.488</b>	<b>1.29</b>	<b>0.161</b>	<b>0.087</b>	<b>0.040</b>	<b>0.013</b>	<b>0.026</b>	<b>0.0111</b>	<b>0.0044</b>	<b>0.0030</b>	<b>0.0014</b>
<b>SE</b>	<b>0.177</b>	<b>0.282</b>	<b>0.74</b>	<b>0.093</b>	<b>0.050</b>	<b>0.023</b>	<b>0.008</b>	<b>0.015</b>	<b>0.0064</b>	<b>0.0026</b>	<b>0.0017</b>	<b>0.0008</b>
<b>CV</b>	<b>8%</b>	<b>11%</b>	<b>26%</b>	<b>15%</b>	<b>12%</b>	<b>11%</b>	<b>8%</b>	<b>19%</b>	<b>13%</b>	<b>12%</b>	<b>18%</b>	<b>15%</b>

### Bioanalysis and PK results

<sup>3</sup>H-HA and <sup>14</sup>C-CS related radioactivity was easily detected and quantified in plasma and knee articulation throughout the study, with signals well above the instrumental detection limits (Tables 5–7). The variations are also expressed from curves (Figures 15 and 16).

Moderate interanimal variability among the concentrations measured was observed. CV values for plasma concentrations ranged from 5% and 35% and from 8% to 26%, respectively, for <sup>3</sup>H-HA and <sup>14</sup>C-CS, and CV values for knee concentrations ranged from 9% to 36% for <sup>3</sup>H-HA and from 28% to 34% for <sup>14</sup>C-CS. The radioactivity related to <sup>3</sup>H-HA and <sup>14</sup>C-CS was quantifiable from 0.25 hour

to 336 hours after the end of administration in plasma, and from 6 hours to 336 hours in the knee.

Plasma radioactivity levels were quantifiable at all collection time points in this study, but at concentrations that were much lower than in the knee articulation (at the site of injection). Plasma concentrations represented approximately 1% and 6% of knee concentrations for <sup>3</sup>H-HA and <sup>14</sup>C-CS related radioactivity, respectively, and, based on AUC values, plasma exposure to <sup>3</sup>H-HA and <sup>14</sup>C-CS related radioactivity represented approximately 5.21% and 0.8% of knee exposure.

<sup>14</sup>C-CS terminal t<sub>1/2</sub> value was similar in the knee and in plasma. This suggests that the rate of disappearance of CS from the injection site corresponds to the absorption rate from the injection site

**Table 7**  
Individual concentration of tritium-labeled hyaluronic acid ( $^3\text{H}$ -HA) and carbon 14-labeled chondroitin sulfate ( $^{14}\text{C}$ -CS)-related radioactivity ( $\mu\text{g-eq/g}$ ) in knee.

Animal ID	Sampling time (sacrifice)							
	$^3\text{H}$ -HA				$^{14}\text{C}$ -CS			
	6 h	24 h	240 h	336 h	6 h	24 h	240 h	336 h
H23921	362				48.9			
H23922	524				61.7			
H23923	632				84.5			
H23924		13.0*				3.57*		
H23925		160				32.3		
H23926		170				35.4		
H23927			5.67				2.84	
H23928			11.7				5.79	
H23929			8.25				4.66	
H23930				5.44				1.97
H23931				4.56				2.22
H23932				4.82				3.54
<b>Mean</b>	<b>506</b>	<b>165</b>	<b>8.55</b>	<b>4.94</b>	<b>65.1</b>	<b>34</b>	<b>4.43</b>	<b>2.57</b>
<b>SD</b>	<b>136</b>	<b>7.07</b>	<b>3.04</b>	<b>0.453</b>	<b>18.0</b>	<b>2.2</b>	<b>1.49</b>	<b>0.842</b>
<b>SE</b>	<b>79</b>	<b>5.00</b>	<b>1.76</b>	<b>0.262</b>	<b>10.4</b>	<b>1.6</b>	<b>0.86</b>	<b>0.49</b>
<b>CV</b>	<b>27%</b>	<b>4%</b>	<b>36%</b>	<b>9%</b>	<b>28%</b>	<b>6%</b>	<b>34%</b>	<b>33%</b>

\* Not included in calculations because the sample was overturned during preparation.

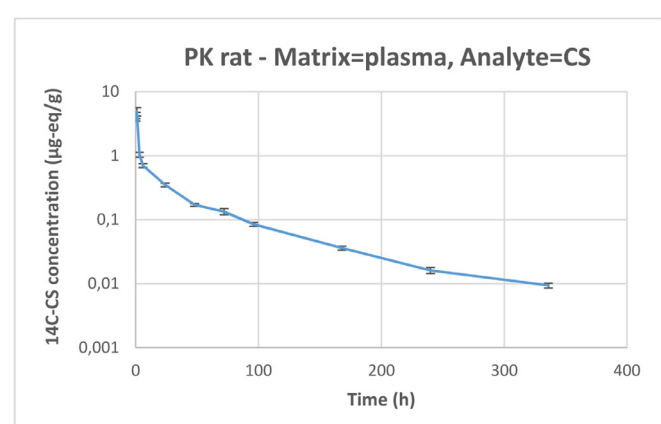
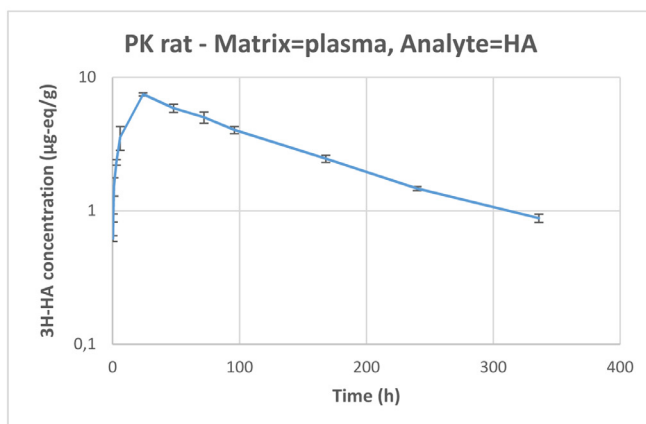
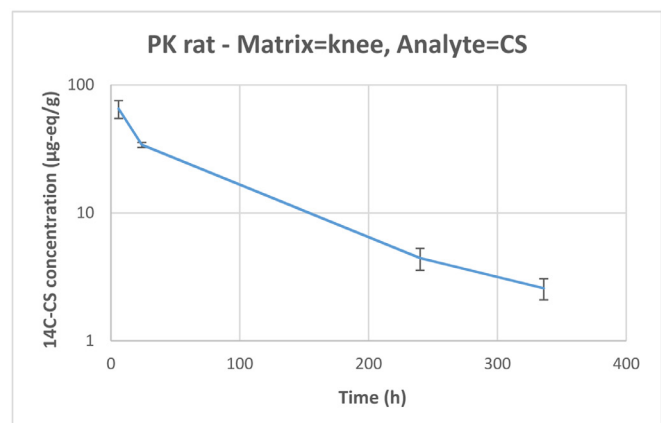
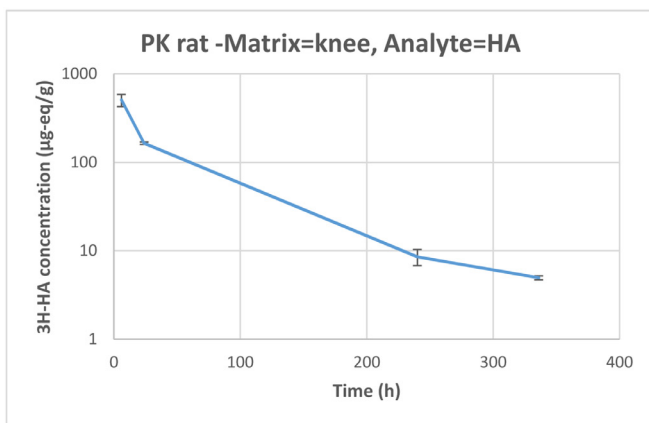


**Figure 15.** Knee and plasma concentration ( $\mu\text{g-eq/g}$ ) of tritium labeled-hyaluronic acid ( $^3\text{H}$ -HA)-related radioactivity over time after single intra-articular administration of 1 mg/animal (equivalent to 0.491 MBq/animal) of HA to male Sprague-Dawley rats (arthritis model) (semi-logarithmic scale). Error bars represent SE. PK = pharmacokinetic.

**Figure 16.** Knee and plasma concentration ( $\mu\text{g-eq/g}$ ) of carbon 14 labeled-chondroitin sulfate ( $^{14}\text{C}$ -CS)-related radioactivity over time after single intra-articular administration of 1 mg/animal (equivalent to 0.261 MBq/animal) of CS to male Sprague-Dawley rats (arthritis model) (semi-logarithmic scale). Error bars represent SE. PK = pharmacokinetic.

into blood, which is a flip-flop case:<sup>30,31</sup> When the  $k_a$  is greater than the  $k_e$ , the elimination phase of the active ingredient profile reflects the input  $k_a$ , rather than the output  $k_e$ . This causes the  $k_a$  to be the rate-limiting step ( $k_e > k_a$ ), making it slower and causing an increase in half-life. This was also the case for HA,

because the elimination phase observed in the plasma profile should reflect the input rate from the IA injection site, rather than the plasma output  $k_e$ .

It was difficult to profile the  $t_{1/2}$  for  $^3\text{H}$ -HA related radioactivity in knees due to the multiphasic trend and the limited

**Table 8**

Pharmacokinetic results. Dose-level: 1 mg/animal.

Analyte	Matrix	Rs <sub>q</sub>	No. of points used to calculate $\lambda_z$	$\lambda_z$	$t_{1/2}$ (90% CI) <sup>a</sup>	$T_{max}$	$C_{max}$	C0	AUC <sub>0-t</sub>	AUC <sub>0-∞</sub>	AUC <sub>t-∞</sub> extrapolated
				1/h	h						
HA	Knee	0.957	3	0.0061	114 (101–131)	6	na	736	21,223	21,647	2
			2	0.0053	131 (77–441)				nc	nc	nc
HA	Plasma	0.995	4	0.0088	79 (57–130)	24	7.47	na	989	1127	12
			2	0.0054	129 (102–174)				nc	nc	nc
CS	Knee	0.989	3	0.0085	82 (69–99)	6	na	80.9	4746	5051	6
			2	0.0056	125 (67–845)				nc	nc	nc
CS	Plasma	0.971	4	0.0079	88 (74–109)	1	4.90	na	39.8	40.8	3
			2	0.0056	124 (87–218)				nc	nc	nc

CS = chondroitin sulfate; HA = hyaluronic acid; na = not applicable; nc = not calculated; Rs<sub>q</sub> = R-squared;  $\lambda_z$  = elimination time constant;  $t_{1/2}$  = half-life; CI = confidence interval; C0 = concentration at time zero (extrapolated);  $C_{max}$  = maximal concentration;  $T_{max}$  = time for maximal reading; AUC = area under the curve.

<sup>a</sup> Calculated using R version 3.6.1. (R Foundation for Statistical Computing, Vienna, Austria).

number of sampling time points available; it is apparently shorter than in plasma if the 3 last time points: 24 hours, 240 hours, and 336 hours are used in the calculation. But looking at the profile of the curve, the terminal elimination phase had probably not yet been reached after 24 hours and the true  $t_{1/2}$  would be better represented by the time point at 240 hours and 336 hours, excluding the 24-hour time point. Therefore, based on the 2 latest points, 240 hours and 336 hours, mean (90% CI) half-life in knee joint and plasma were found to be 131 hours (90% CI, 77–441 hours) and 129 hours [90% CI, 102–174 hours] for <sup>3</sup>H-HA, and 125 hours [90% CI, 67–845 hours] and 124 hours [90% CI, 87–218 hours], respectively, for <sup>14</sup>C-CS.

Maximum concentrations in plasma were reached at 1 hour and 24 hours after IA administration for <sup>3</sup>H-HA and <sup>14</sup>C-CS related radioactivity, respectively. A large difference was observed between concentrations in the joint and in plasma. For <sup>3</sup>H-HA, the joint concentration to plasma concentration ratio was 142 at 6 hours, then became smaller over time: 22 at 24 hours, 5.8 at 240 hours and 5.6 at 336 hours. For <sup>14</sup>C-CS, the ratio was 92 at 6 hours, 97 at 24 hours, 273 at 240 hours and 272 at 336 hours. In both cases, the ratio was stable between 240 hours and 336 hours, although evolving in opposite directions. Logically, the low ratio for HA could result from the presence of HA in the synovial fluid. And the much higher ratio reached for CS could result from a penetration and fixation of CS inside the cartilage as the plasma-eliminated fraction becomes very small over time. PK results are summarized in Table 8.

## Discussion

### MIA rat OA model

Altogether, the OA induced on this MIA rat model appeared to satisfactorily mimic OA in humans. The disease status can be rapidly induced in animals, thus making this model attractive. There are some recognized concerns about using this type of approach. Firstly, according to the literature and to our observations, OA induced in rats by MIA injection, progressed very fast, when compared with human OA, and this appeared to be a potential limitation to study the HCS clinical efficacy in MIA treated animals, as response to viscosupplementation could be delayed as in humans.<sup>6–8</sup> Secondly, and related to the clinical end point normally adopted, the evaluation of pain that can only be indirectly assessed from the impaired motion in animals.

Our approach to assessing the development of OA symptoms in animals was based on:

- Physical performance tests, as automated infrared sensor, using measurable parameters such as rearing scores (spontaneous exercise), represent experimental conditions in which low stress-

related environments are observed during the evaluation of motor activity in rats.

- Knee joint histology: Several MIA rat studies indicate an important loss of GAGs in cartilage, together with chondrocyte necrosis, which are key characteristics of OA in humans. At the advanced stage of MIA-induced OA, the integrity of the subchondral bone is compromised (bone marrow loss, then collapse). In such a situation, cartilage cannot be restored or healed by any available treatment. In our OA model, no collapse was detected up to day 22.

An equivalence to the Kellgren-Lawrence radiological scale (I–IV) used in humans is of course impossible to establish. Radiology is not an available approach for rats in comparison with humans. Other limitations might be related to the number of animals involved in both treated and control animals. But our intention was to use a reduced number of animals as the MIA model was clearly established in the literature.

### PK compared results

Previously published data indicate that the plasma half-life of intravenously injected <sup>3</sup>H-HA in humans ranged between 2.5 and 4.5 minutes.<sup>32</sup> This PK analysis in MIA rats showed that the radioactivity coming from HA and/or CS stays in the joint, with a half-life of nearly 5 days (around 120 hours). Similar terminal  $t_{1/2}$  values were detected in plasma following the IA injection, thus indicating that via this administration route, the plasma half-life is mainly influenced by the release rate from the injection site and not by the systemic clearance rate. This first important result in our study is that HA, but also CS, despite its smaller average MW, are very slowly released from the IA injection site, resulting in a half-life of several days. The second important result indicates that much higher concentrations of labeled HA and CS related material were observed at the injection site than in plasma for the entire duration of the observation period.

No PK data were available in the literature concerning IA injection of CS, but we found several previous studies describing IA administration of HA. After IA in rabbits, HA residence time has been described as relatively short, with half-life values of 10.2 hours for low MW HA (90 kDa) versus 13.2 hours for very high MW HA (>6 MDa).<sup>33</sup> This confirmed that PK properties of HA were not strongly dependent on MW. In another study in rabbits,<sup>34</sup> the HA half-life was 15.8 hours in synovial fluid and 17.5 hours in plasma. Cross-linked HA materials have been specifically designed to extend this residence time by increasing the resistance of HA to metabolism (hydrolysis). High MW was considered to prolong the  $t_{1/2}$  by delaying filtration through the synovial membrane (synovium)<sup>35</sup> before reaching the lymph and then the blood circulation system.<sup>36,37</sup> The half-life of Hylan GF-20 (Synvisc; Sanofi-Aventis US, Bridgewater,

New Jersey) was found to be 1.5 day (36 hours) for the hylan A fraction (>6 MDa) and 8.8 days (211 hours) for the hylan B cross-linked fraction, from joint sampling.<sup>38</sup> These results were not far from those measured in this study. This contributes to establishing that plasmatic exposure and systemic clearance of HA are influenced by the absorption rate from the site of injection and that a significant part of injected HA remains in the joint area for a long time before being eliminated.

Unlike HA, CS is not present in the normal synovial fluid, but it is abundant in the cartilage matrix. The ability of CS to fix onto synoviocytes or chondrocytes and stimulate HA production has been proved in vitro,<sup>39–42</sup> but the ability of IA-administered CS to deeply penetrate the cartilage has not yet been demonstrated. CS clearance from the IA injection site may occur via synovial membrane filtration and lymph drainage, as for HA. But other pathways (ie, via blood capillaries in the synovium and subchondral bone) may not be excluded. In plasma, we measured <sup>3</sup>H and <sup>14</sup>C radioactivity probably coming essentially from degradation by products in the initial radio-labeled, active, principle GAGs, following hyaluronidases or CS hydrolases. These elimination pathways are the same for the exogen GAGs as for the endogen GAGs, due to their molecular identity. There is great similarity between the HA and CS degradation processes. The main difference for CS is the need to eliminate the sulfate compounds through additional steps.<sup>43</sup>

Compared with other alternative administration routes, such as oral or intravenous, the IA injections of GAGs offers the advantage of producing higher concentrations at the target site of action along with low systemic exposure, thus avoiding loss of the larger fraction of the administered dose due to poor absorption and/or fast systemic metabolism.<sup>44</sup>

We believe that the ability of GAGs to fix on tissues and cell receptors contributing to the biological equilibrium inside the joint area<sup>39–42</sup> is largely influenced by the local GAGs concentration and the length of exposure. In consequence, the effect of HA and CS on cartilage degradation, being more complex than a purely mechanical role,<sup>2,44</sup> may be positively and largely influenced by their PK properties. This PK study involving IA administration of HA and CS associated in the same formulation demonstrated that these 2 GAGs have a very similar residence time, with half-lives of approximately 5 days, despite their difference in MW. Clearly, combining CS with HA in the same viscosupplement offers several advantages,<sup>45</sup> and on the clinical side in human OA, at least 2 studies have already proposed results in favor of IA preparations associating HA and CS.<sup>46,47</sup> Due to its steric size, high MW HA is supposed to stay in the synovial fluid<sup>36,37</sup> rather than to easily penetrate the tissue meshwork. For the small CS molecules that stay, surprisingly, in the joint, the probability of penetration into tissue seems high, and cartilage could be the best candidate as tissue receptor, but other trials are necessary to confirm this hypothesis.

## Conclusions

After local administration of sodium MIA to Sprague-Dawley rats (to obtain an animal model for arthritis), impairments of spontaneous motor activity were observed from day 4 to day 15. The clinical signs were considered to be related to MIA administration and the histology investigation of the cartilage confirmed synovium inflammation, great loss of GAGs, chondrocyte necrosis, presence of clefts, and later modifications in the subchondral bone, all of which are symptoms and effects associated with human OA. Therefore, the OA disease status was considered to have been correctly reproduced in the animals used in this study.

The PK study allowed us to demonstrate a relatively long half-life for both HA and CS (about 5 days), estimated at 129 hours and 124 hours in the plasma versus 131 hours and 125 hours in

the knee joint, respectively. The difference in molecular weight between HA and CS does not seem to have had a large influence in the half-life according to results obtained in this study. Another important aspect of the results is the concentration levels obtained for HA and CS. These were much higher in the joint than in plasma. Particularly for CS at 240 hours and 336 hours postinjection, when the concentration was found to be more than 270 times higher in the joint than in plasma. Globally, this study leads to the conclusion that IA administration of GAGs led to PK behavior characterized by prolonged residence inside the joint, allowing induced long-term beneficial effects, and only a slow release in plasma.

## Declaration of Competing Interest

Massimiliano Fonsi, Abdel-Ilah El Amrani, and Frédéric Gervais are employees of Citoxlab France, which received financial support for the conduct of this research from LCA Pharmaceutical. Patrice Vincent is an employee and shareholder of LCA Pharmaceutical. The authors have indicated that they have no other conflicts of interest regarding the content of this article.

## Acknowledgments

The authors thank Pauline Rousseau, PharmD (Citoxlab, France), for her expertise in the preparation of the final radio-labeled HCS solution and Joanna Moore, ELS (Citoxlab France), for her assistance in the preparation of the manuscript.

## Contributors

Contribution of each author to the study and the publication was:

MF: Each point from study design to the final writing of the article (except for histology)

PV: Each point of the study as sponsor representative, literature search, data interpretation, and to the writing of the article up to the final corrections

AEA: Each point from study design to data collection and interpretation (except for PK aspects), and to the writing of the article

FG: Major actor for data collection on animals, including histology pictures and interpretation

## References

1. Reid MC. Viscosupplementation for osteoarthritis: a primer for primary care physicians. *Adv. Ther.* 2013;30(11):967–986.
2. Altman RD, Manjoo A, Fierlinger A, Niazi F, Nicholls M. The mechanism of action of hyaluronic acid treatment in the osteoarthritis of the knee: a systematic review. *BMC Musculoskeletal Disorders.* 2015;16:321. doi:10.1186/s12891-015-0775-z.
3. Hascall VC, Laurent TC. Hyaluronan: Structure and Physical Properties Glycoforum / Science of Hyaluronan 1 - <http://www.glycoforum.gr.jp/hyaluronan>.
4. Fox AJS, Bedi A, Rodeo SA. The Basic Science of Articular Cartilage: Structure, Composition, and Function. *Sports Health [Orthopaedics]*. 2009;1(6):461–468. doi:10.1177/1941739109350438.
5. Chevalier X, Richette P. Cartilage articulaire normale: anatomie, physiologie, métabolisme, vieillissement. *EMC Appareil Locomoteur 14-003-A-10 / EMC-Rhumatologie Orthopédie.* 2005;2:41–58 (Elsevier) doi:10.1016/j.emcrho.2004.10.005.
6. Richette P. Viscosupplémentation au genou – hyaluronan for knee osteoarthritis. *Revue du rhumatisme monographies.* 2016;83:158–161 doi:10.1016/j.monrhu.2016.03.005.
7. Maheu E, Rannou F, Reginster JY. Efficacy and safety of hyaluronic acid in the management of osteoarthritis : Evidence from real-life setting trials and surveys. *Seminars in Arthritis and Rheumatism.* 2016;45:528–533. <http://dx.doi.org/10.1016/j.semarthrit.2015.11.008>.
8. Maheu E, Bannuru RR, Herrero-Beaumont GH, Allali F, Bard H, Migliore A. Why should we definitely include intra-articular hyaluronic acid as a therapeutic option in the management of knee osteoarthritis: Results of an extensive critical literature review. *Seminars in Arthritis and Rheumatism.* 2018;48:563–572. <http://dx.doi.org/10.1016/j.semarthrit.2018.06.002>.

9. Little CB, Smith MM. Animal models of osteoarthritis. *Current Rheumatology Reviews*. 2008;4(3):1–8.
10. Guingamp C. *Etudes morphologique, fonctionnelle, et biochimique de modèles d'arthrose expérimentale chez le rat: Intérêts du modèle d'arthrose induite par injection de iodoacétate*. Université, Nancy 1; 1999 PhD thesis.
11. Guingamp C, Gegout-Pottie P, Philippe L, Terlain B, Netter P, Gillet P. Mono-iodoacetate-induced experimental osteoarthritis: a dose-response study of loss of mobility, morphology, and biochemistry. *Arthritis Rheum*. 1997 Sep;40(9):1670–1679.
12. Janusz MJ, Hookfin EB, Heitmeyer SA, Woessner JF, Freemont AJ, Hoyland JA, Brown KK, Hsieh LC, Almstead NG, De B, Natchus MG, Pikul S, Taiwo YO. Moderation of iodoacetate-induced experimental osteoarthritis in rats by matrix metalloproteinase inhibitors. *Osteoarthritis and Cartilage*. 2001;9:751–760. [www.idealibrary.com](http://www.idealibrary.com).
13. Guzman RE, Evans MG, Bove S, Morenko B, Kilgore K. Mono-iodoacetate-Induced Histologic Changes in Subchondral Bone and Articular Cartilage of Rat Femorotibial Joints: An Animal Model of Osteoarthritis. *Toxicologic Pathology*. 2003;31:619–624.
14. Saito R, Sekiya I, Ozeki N, Nakagawa Y, Udo M, Yanagisawa K, Tsuji K, Muneta T. Strenuous Running enhances Degeneration of Articular Cartilage in a Rat MIA-induced Arthritis Model - <http://prgmobileapps.com/AppUpdates/ors2015/Abstracts/abs445.html>.
15. Peng Z, Vääränen J, Fagerlund KM, Rissanen JP, Bernoulli J, Halleen JM, Morko J. Characterization of Monosodium Iodoacetate Induced Osteoarthritis in Rat Knee, including Patellofemoral and Tibiofemoral Joints - MO0198 - Pharmatest Services Ltd, Turku, Finland - [www.pharmatest.com](http://www.pharmatest.com).
16. Ferland CE, Pailleux F, Vachon P, Beaudry F. *Determination of specific neuropeptides modulation time course in a rat model of osteoarthritis pain by liquid chromatography ion trap mass spectrometry - Catherine Estelle FERLAND-LEGAULT*. Dawley: Université de Montreal: Caractérisation d'un modèle animal de douleur articulaire associée à l'arthrose du genou chez le rat Sprague; 2011 PhD thesis.
17. Ferland CE, Laverty S, Beaudry F, Vachon P. Gait analysis and pain response of two recent models of osteoarthritis. *Pharmacology, Biochemistry and Behavior*. 2011;97:603–610.
18. Liu P, Okun A, Ren J, Guo RC, Ossipov MH, Xie J, King T, Porreca F. Ongoing Pain in the MIA Model of Osteoarthritis. *Neurosci Lett*. 15 April 2011;493(3):72–75.
19. Mannelli LdC, Bani D, Bencini A, Brandi ML, Calosi L, Cantore M, Carossino AM, Ghelardini C, Valtancoli B, Failli P. Therapeutic Effects of the Superoxide Dismutase Mimetic Compound MnIIIme2DO2A on Experimental Articular Pain in Rats. *Hindawi Publishing Corporation Mediators of Inflammation*. 2013;1–11.
20. Benschop RJ, Collins EC, Darling RJ, Allan BW, Leung D, Conner EM, Nelson J, Gaynor B, Xu J, Wang XF, Lynch RA, Li B, McCarty D, Oskins JL, Lin C, Johnson KW, Chambers MG. Development of a novel antibody to calcitonin gene-related peptide for the treatment of osteoarthritis-related pain. *Osteoarthritis and Cartilage*. 2014;22:578–585.
21. Naveen SV, Ahmad RE, Hui WJ, Suhaeb AM, Murali MR, Shanmugam R, Kamarul T. Histology, Glycosaminoglycan Level and Cartilage Stiffness in Monoiodoacetate-Induced Osteoarthritis: Comparative Analysis with Anterior Cruciate Ligament Transection in Rat Model and Human Osteoarthritis. *Int. J. Med. Sci.*. 2014;11.
22. Calado GP, Lopes AJO, Costa Junior LM, Lima FdCA, Silva LA, Pereira WS, do Amaral FMM, Garcia JBS, Cartágenes MdSdS, Nascimento FRF. Chenopodium ambrosioides L. Reduces Synovial Inflammation and Pain in Experimental Osteoarthritis. *PLOS ONE November*. 2015;2:1–18.
23. Jain A, Singh R, Singh Sau, Singh San. Diacerein protects against iodoacetate-induced osteoarthritis in the femorotibial joints of rats. *The Journal of Biomedical Research*. 2015;29(5):405–413. open access at PubMed. [www.jbr-pub.org](http://www.jbr-pub.org).
24. Ruehl-Fehlert C, Kittel B, Morawietz G, Deslex P, Keenan C, Mahrt CR, Nolte T, Robinson M, Stuart BP, Deschl U. Revised guides for organ sampling and trimming in rats and mice - Part 1. *Exp. Toxicol. Pathol*. 2003;55:91–106.
25. Kittel B, Ruehl-Fehlert C, Morawietz G, Klapwijk J, Elwell MR, Lenz B, O'Sullivan MG, Roth DR, Wadsworth PF. Revised guides for organ sampling and trimming in rats and mice - Part 2. *Exp. Toxicol. Pathol*. 2004;55:413–431.
26. Morawietz G, Ruehl-Fehlert C, Kittel B, Bube A, Keane K, Halm S, Heuser A, Hellmann J. Revised guides for organ sampling and trimming in rats and mice - Part 3. *Exp. Toxicol. Pathol*. 2004;55:433–449.
27. Svanovsky E, Velebný V, Laznickova A, Laznickek Ml. The effect of molecular weight on the biodistribution of hyaluronic acid radiolabeled with <sup>111</sup>In after intravenous administration to rats. *Eur J Drug Metab Pharmacokinet*. 2008;33(3):149–157.
28. Yamane Y, Ishide N, Kagaya Y, Takeyama D, Shiba N, Chida M, Sekiguchi Y, Nozaki T, Ido T, Shirato K. Quantitative double-tracer autoradiography with tritium and carbon-14 using imaging plates: Application to myocardial metabolic studies in rats. *J Nucl Med*. 1995;36:518–524.
29. Cohen J. *Statistical power analysis for the behavioral sciences*. (2nd edition). Hillsdale, NJ: Lawrence Erlbaum Associates; 1988.
30. Derendorf H, Höllmann H, Grüner A, Haack D, Gyselby G. Pharmacokinetics and pharmacodynamics of glucocorticoid suspensions after intra articular administration. *Clin Pharmacol Ther*. 1986;39(3):313–317.
31. Yanez JA, Remsberg CM, Syare CL, Forrest ML, Davies NM. Flio-flop pharmacokinetics – delivering a reversal of disposition: challenges and opportunities during drug development. *Future Science Ltd, Therapeutic Delivery*. 2011;2(5):643–672.
32. Fraser JRE, Laurent TC, Pertoft H, Baxter E. Plasma clearance, tissue distribution and metabolism of hyaluronic acid injected intravenously in the rabbit. *Biochem J*. 1981;200:415–424.
33. Brown TJ, Laurent UBG, Fraser JRE. Turnover of Hyaluronan in Synovial Joints: Elimination of Labelled Hyaluronan from the Knee Joint of the Rabbit. *Experimental Physiology*. 1991;76:125–134.
34. Lyndenhayn K, Heilmann HH, Niederhausen T, Walther HU, Pohlentz K. Elimination of Tritium-Labelled Hyaluronic Acid from Normal and Osteoarthritic Rabbit Knee Joints. *Eur J Clin Biochem*. 1997;35(5):355–363.
35. Smith MD. The Normal Synovium. *The Open Rheumatology Journal*. 2011;5(Suppl 1:M2):100–106.
36. Coleman PJ, Scott D, Mason RM, Levick JR. Role of hyaluronan chain length in buffering interstitial flow across synovium in rabbits. *Journal of Physiology*. 2000;526(2):425–434.
37. Levick JR, Coleman PJ, Scott D, Mason RM. Secretory Regulation *in vivo* Molecular Reflection & Hydraulic Roles of Synovial Hyaluronan. In: Kennedy J, Phillips G, Williams P, Hascall V, eds. *Hyaluronan*, 2, Woodhead Publishing Limited; 2002:329–336.
38. Larsen NE, Dursema HD, Pollak CT, Skrabut EM. Clearance kinetics of a hylan-based viscosupplement after intra-articular and intravenous administration in animal models. *J Biomed Mater Res Part B*. 2012;100B:457–462 2012.
39. Moreland LW. Intra-articular hyaluronan (hyaluronic acid) and hylans in the treatment of osteoarthritis: mechanism of action. *Arthr Res Ther*. 2003;5:54–67. doi:10.1186/ar623.
40. Gosh P, Guidolin D. Potential Mechanism of Action of Intra-articular Hyaluronan Therapy in Osteoarthritis: Are the Effects Molecular Weight Dependent? *Seminars in Arthritis and Rheumatism*. 2002;32(1):10–37.
41. Vitanzo PC, Sennett BJ. Hyaluronans: Is Clinical Effectiveness Dependent on Molecular Weight? *The American Journal of Orthopedics*. 2006;September 2006:421–428.
42. David-Raoudi M, Deschrevel B, Leclercq S, Galéra P, Boumediene K, Pujol JP. Chondroitin Sulfate Increases Hyaluronan Production by Human Synoviocytes Through Differential Regulation of Hyaluronan Synthases – Role of p38 and Akt. *Arthritis & Rheumatism*. 2009;60(3):760–770. doi:10.1002/art24.302.
43. Yamada S. Catabolism of chondroitin sulfate. *Cellular & Molecular Biology Letters*. 2015;20:196–212.
44. Loeser RF. Molecular mechanisms of cartilage destruction: Mechanics, inflammatory mediators, and aging collide. *Arthritis Rheum*. 2006;54(5):1357–1360.
45. David-Raoudi M, Menchini R, Pujol JP. Glyco-Forum section - For intra articular delivery of chondroitin sulfate. *Glycobiology*. 2009;19(8):813–815 cwp069.
46. Henrotin Y, Hauzeur JP, Bruel P, Appelboom T. Intra-articular use of a medical device composed of hyaluronic acid and chondroitin sulfate (Structovial CS): effects on clinical, ultrasonographic and biological parameters. *BMC Research Notes*. 2012;5(407):1–7.
47. Rivera F, Bertignone L, Grandi G, Camisassa R, Comaschi G, Trentini D, Zanone M, Teppex G, Vasario G, Fortina G. Effectiveness of intra-articular injections of sodium hyaluronate – chondroitin sulfate in knee osteoarthritis: a multicentre prospective study. *J Orthopaed Traumatol*. 2016;17:27–33. doi:10.1007/s10195-015-0388-1.